JOURNAL OF MATERIALS SCIENCE **37** (2002) 3705 – 3713

The effect of processing variables on the microstructures and properties of aluminum brazed joints

H. NAYEB-HASHEMI, M. LOCKWOOD
Department of Mechanical, Industrial and Manufacturing Engneering, Northeastern University, Boston, MA 02115, USA

Aluminum brazed joints are used extensively in the automotive and aircraft industries. In order to insure the integrity of the bond, the effects of processing variables on the quality of the bond must be understood. The effects of brazing period and joint thickness on the microstructure, tensile properties, microhardness and micromechanisms of failure of two aluminum alloy 3003 plates connected by a layer of 4047 aluminum filler material were investigated. It was found that the amount of aluminum-silicon eutectic microstructure in the reaction zone decreased with increasing brazing period and decreasing joint thickness. This was attributed to silicon diffusion from the joint material and dissolution of base metal and its entrance into the liquid joint. The amount of shrinkage porosity in the reaction zone was found to increase with increasing brazing period due to base material solutioning. The ultimate tensile strength of joints decreased with increasing brazing period and decreasing joint thickness. This was attributed to the joint microstructure and shrinkage porosity formed in the joint. Shrinkage porosity was found to be the primary cause of decreased joint strength. Joints with 10 minutes brazing period failed within the base material, while for brazing periods greater than 10 minutes, joints failed within the aluminum-silicon eutectic microstructure of the reaction zone. This indicated that the joint strength was greater than the base material for joint with brazing period of 10 minutes. Finite element analysis was performed to determine the effect of joint material yield strength and joint thickness on the stress and strain field in the brazed joint. Finite element analysis results supported experimental observations.

1. Introduction

Aluminum components are often joined together by brazing. Examples of aluminum-brazed joints can be found in automotive, aerospace and electronic industries, etc. These joints are often subjected to complex loading conditions. It is therefore essential to understand the effects of processing variables on the joint mechanical properties in order to insure their safe design.

Various processes have been developed for joining materials. The underlying principal in most permanent metal joining processes is based on bringing two pieces of metal within 4 Å of each other [1]. Inter-atomic attraction will then bind them together in a permanent metallic bond. In the case of brazing or soldering, this is accomplished by "wetting" the metals to be joined with molten metal, which on cooling forms a joint. If the temperature of the wetting metal is above 426°C (800°F), the process is called brazing and the molten metal is called brazing filler metal. If the temperature is below 426°C (800°F), the process is called soldering and the molten metal is called solder [1–3].

There is numerous aluminum brazing methods. In the present research, furnace brazing was used to make the aluminum joints. Furnace brazing is the second most popular method of brazing aluminum. In furnace brazing, the joining surfaces are fluxed, filler metal is positioned, and the parts are assembled and fixtured. The assembly is then usually heated in a pre-heated oven to drive the moisture or alcohol out of the flux. The assembly is then placed in a furnace, which is at the brazing temperature, and usually remains there for 3 to 5 minutes after it has reached brazing temperature [1].

Most early brazing research was based on steel base metals brazed with silver, copper, and various alloys. These studies have reported the failure mechanisms and stress distributions in steel butt brazed joints subjected to various loading conditions [4–10]. Saxton *et al.* [6–8] investigated the deformation and failure of brazed steel rods using various filler materials. The failure of the brazed joints was observed to occur within the joints rather than at the braze interface. This indicated that interfacial defects (compound formation, poor adhesion, and so forth) were not important in the failure process. The failure of joints was attributed to formation of micropores in joints. The joints were observed to fail when these micropores grew to coalescence under the influence of applied loads. The criterion for unstable growth was influenced by both the base metal yield strength and

the joint geometry. Yielding of the base metal decreased triaxial tension within the braze metal. Decreasing triaxiality resulted in higher axial strains within the joint causing void growths and coalescence. When the base metal remained elastic during loading, triaxial tension alone produced void growths and coalescence.

Sasabe [9] analyzed the effect of joint thickness on fatigue crack initiation and fatigue crack growth rate of a brazed butt joint of carbon steel and stainless steel brazed with pure copper with and without an artificial defect. For specimens without an artificial defect, smaller joint clearance created greater constraining influence that delayed plastic deformation and crack initiation. This resulted in longer crack initiation time, which resulted in a longer fatigue life of the joint.

There are a number of papers reporting the effects of the processing variables on the aluminum-brazed joints properties [11–21]. Woods *et al*. [16] investigated the flow of aluminum-silicon brazing filler metal. It was concluded that flow of aluminum-silicon brazing alloy is governed by a mechanism of local eutectic melting. Furthermore, it was found that increasing the thickness of the cladding layer increased brazing metal flow leading to an increase in base material melting and mixing with the filler material.

Schmatz [20] investigated grain boundary penetrations of aluminum-silicon braze clad into the underlying base material. The study compared penetration susceptibility of several aluminum alloy types, including 3004 and 3003. During brazing, the thin layer of clad melts, and depending on the brazing temperature and time, some of the base material will liquefy. When this occurs uniformly it is called base solutioning or erosion. When it occurs preferentially at grain boundaries, it is commonly called silicon grain boundary penetration. This was attributed to the silicon diffusion from the filler material to the base material grain boundaries.

The literature survey for this research clearly indicated lack of understanding of the effects of the processing variables such as initial joint thickness, and brazing period on the joint microstructure and mechanical properties of the brazed joint. The purpose of this work is to find the effect of brazing period and joint thickness on the microstructure, tensile properties, and micromechanisms of failure of aluminum brazed butt joints.

2. Experimental procedure

2.1. Materials

A brazed joint consisted of two aluminum alloy 3003 plates connected by a rod of aluminum alloy 4047 filler metal. Aluminum alloy 3003 was chosen as the base material due to the ease with which it could be furnace brazed with conventional fluxes. Aluminum alloy 4047 was chosen as the joint material because it has a short melting range (temperature difference between the liquidus and solidus), and because it is commonly used to furnace braze aluminum alloy 3003. The most effective flux found for creating the joints in this study was a non-corrosive aluminum flux. It is a stable mixture of NOCOLOK© flux patented by Alcan International and an organic compound. It is applied as flux slurry. Table I shows the compositions of the base and filler materials.

TABLE I Base material and joint material composition (wt%)

Alloy	Si	Fe	Cu	Mn	Mg	Zn	Al
3003	0.6	0.7	0.05–0.20	1.0–1.5	0.0	0.1	Bal.
4047	11.0–13.0	0.8	0.3	0.15	0.1	0.2	Bal.

2.2. Specimens preparation

The specimens were prepared from a plate of 3003 with thickness of 3.18 mm. Strip of aluminum plates with width of 25.4 mm and length of 50.8 mm were cut from the plate and prepared for brazing. The end sections of the plates were machined and cleaned in acetone using an ultrasonic cleaner. The plates were then assembled in a stainless steel fixture and prepared for brazing. Shims of various thickness was inserted at the edge of the two plates to control the braze thickness. The fixture was equipped with two leaf springs, which squeezes the two plates and shims together for the entire brazing period, even with some base material dissolution. This system ensured manufacturing joints with a specified braze joint thickness. The brazing surfaces were coated with the flux and the filler material was placed in the top of the joint. The assembly was then placed in a furnace at 640°C. Brazing period of 10, 20, 30, and 40 minutes was used to join plates. Specimens were then removed from the oven and cooled to the room temperature.

2.3. Tensile tests

Fig. 1 shows the schematic diagram of specimens used for tensile tests. The specimens' surfaces were polished to remove oxides and any filler material left on the surface of the specimens. ASTM standard E8-99 [22] was followed for all tensile tests. In addition to brazed

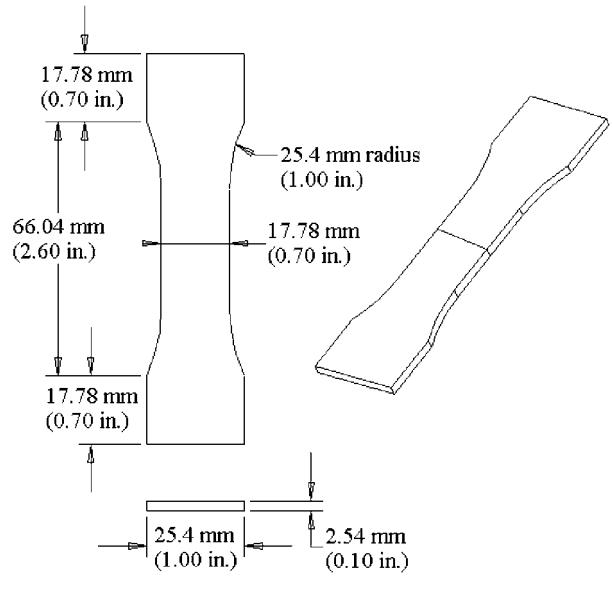

Figure 1 Schematic diagram of tensile test specimens.

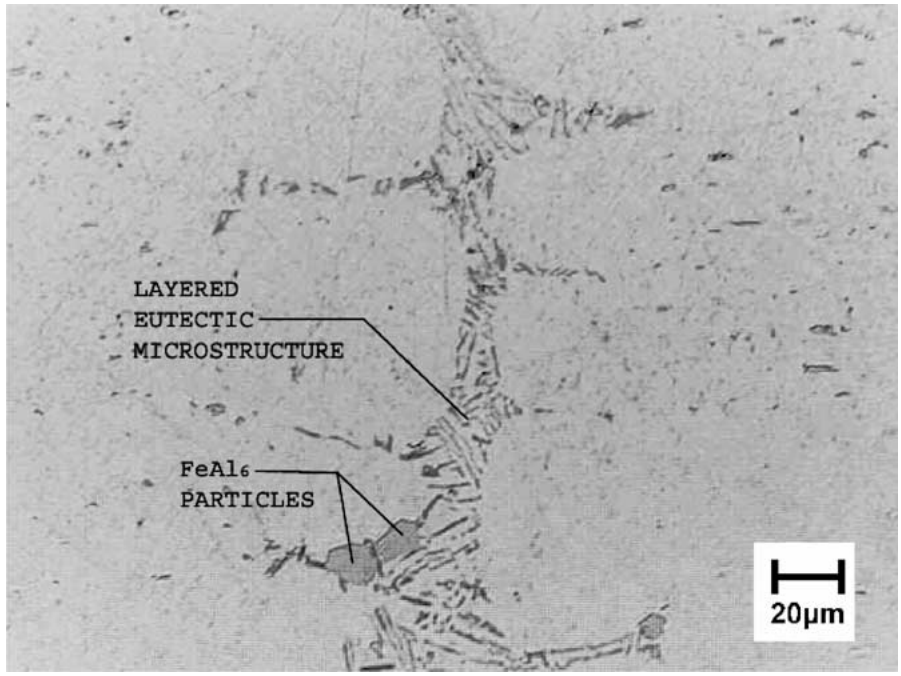

Figure 2 Photomicrograph of a 10 min brazed joint with a joint thickness of 0.00 mm.

specimens, the mechanical properties of the based material and filler material were measure in the as received condition and after exposing them to the same brazing duration and temperature.

3. Results and discussions

3.1. Microstructure of the brazed joint

Fig. 2 shows a typical photomicrograph of a 10-minute brazed joint with a joint thickness of 0.00 mm. Dendrites of aluminum solid solution (light gray) and aluminum-silicon eutectic matrix (dark) are visible in the reaction zone. In addition several intermetallic compounds of aluminum with Fe, Mn, Cu and Si were found to be dispersed throughout the base material [23]. For this joint, the interface between the joint material and the base material was not clearly defined. Eutectic branches of aluminum-silicon microstructure can be seen penetrating the base material along grain boundaries normal to the joint direction.

Figs 3–6 are photomicrographs of the reaction zone of brazed joints produced with joint thicknesses of

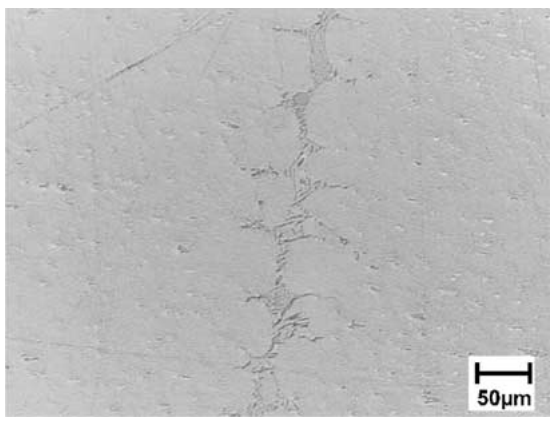

Figure 3 Photomicrograph of a 10 min brazed joint with a joint thickness of 0.00 mm.

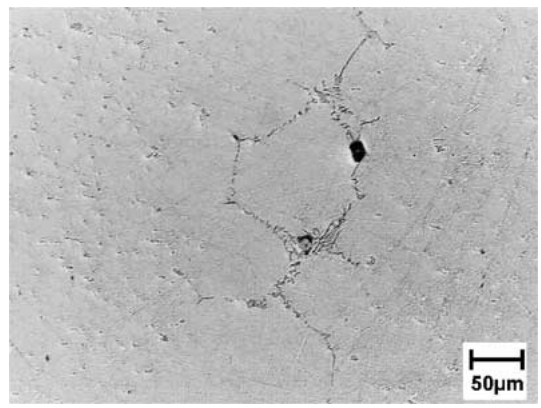

Figure 4 Photomicrograph of a 40 min brazed joint with a joint thickness of 0.00 mm.

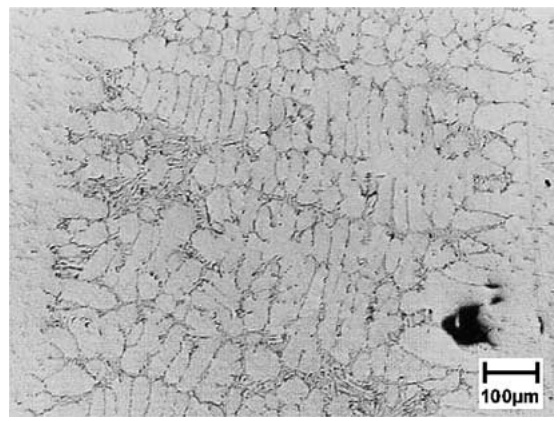

Figure 5 Photomicrograph of a 10 min brazed joint with a joint thickness of 0.254 mm (0.010 in.).

0.00 mm and 0.254 mm (0.010 in.) for 10 and 40 minute brazing periods. The micrographs reveal that as the brazing period increases the amount of eutectic microstructure decreases. This can be attributed to

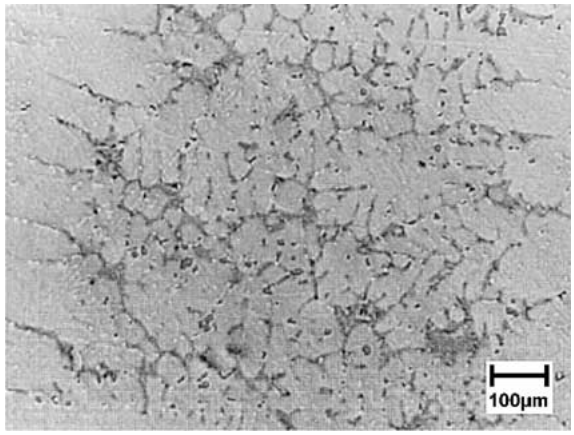

Figure 6 Photomicrograph of a 40 min brazed joint with a joint thickness of 0.254 mm (0.010 in.).

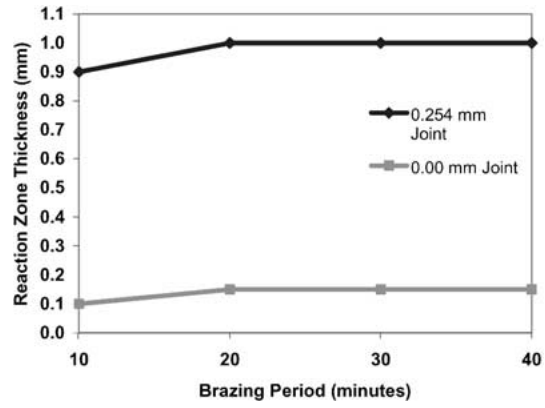

Figure 7 Variation of reaction zone thickness with brazing period.

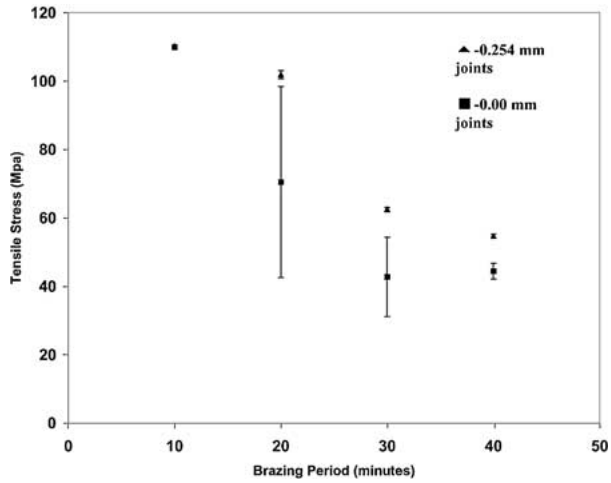

Figure 8 Variation of average ultimate tensile strength with brazing period.

silicon diffusion from the joint material into the base material and dissolution of base material and its entrance to the liquid joint area. Silicon diffusion and base material solutioning cause the joint material to become increasingly hypoeutectic as the brazing period increases. The amount of eutectic microstructure within the reaction zone also appears to increase with increasing joint thickness. This is due to an increased amount of silicon present within the joint with increasing joint thickness. There was no change in the base material microstructure and grain size with increasing of brazing period and joint thickness.

The microstructure of the brazed joint was significantly different in the top and bottom of the joint than in the middle of the joint. For joints with 0.00 mm joint thickness the reaction zone was approximately twice as wide at the top and bottom of the joint than at the middle of the joint. This can be justified considering that the molten filler metal is being drawn into the top of the joint by capillary action, possibly eroding the top edges of the base material in the process. The composition of joint in the top of the joint can thus be considered to be at the hypereutectic composition, while its composition in the middle of the joint could be at hypoeutectic. These variations in the joint compositions could be readily related to the observed developed microstructures. Furthermore, the diffusion rate is higher in the top surface layer than in the bulk material. Similar process occurs in the bottom of joint by presence of more filler material with high Silicon content in the bottom of the joint. The effects of varying reaction zone width and microstructure through the joint on the tensile test results is believed to be minimal because the affected sections were essentially removed by sanding and polishing processes used to prepare tensile specimens.

Fig. 7 shows the reaction zone size vs. the brazing period. The reaction zone was measured by polishing the joint area and measuring the extent of the hypoeutectic microstructure present in the joint area. The reaction zone probably is slightly larger than the measured reaction zone size, due to precipitation of Si from the base material. No exhaustive effort was made to measure the variation of the Silicon concentration in the based material from the joint area and thus establishing a more accurate measurement of the reaction zone size. The results indicate that the reaction zone size initially increases with the brazing period and remain almost constant for brazing period greater than 20 minutes.

3.2. Tensile properties

Table II shows the mechanical properties of the base material subjected to the same temperature and period as the brazing processes. The base material apparently is annealed when subjected to 640°C. However increasing the exposure from 10 minutes to 40 minutes did not further change the mechanical properties of the base material. Fig. 8 shows the average ultimate tensile strength of joints versus brazing period for joint with 0.00 mm and 0.254 mm thickness, with error bars indicating the standard deviation from several tests. It is seen that the average ultimate tensile strength of brazed joints decreases with increasing brazing period. It is observed that increasing the joint thickness from 0.00 mm to 0.254 mm (0.010 in.) improved joint strength when the brazing period was greater than 10 minutes. The strength of brazed joints with 10 minute brazing periods approached the ultimate tensile strength of the base material.

The variation of ultimate tensile strength with the brazing period and joint thickness can be related to the

TABLE II Base material and joint material mechanical properties

Alloy	Furnace temp. (°C)	Brazing period (min)	0.2% offset yield strength (MPa)	Tensile strength (MPa)	Elongation (25.4 mm gage length) (%)	Reduction of cross sectional area (%)	Elastic modulus (GPa)	Poisson's ratio
3003	n/a	As received	144.8	151.7	17	58	70.3	0.33
3003	640	10	38.6	106.9	23	77	70.3	0.33
3003	640	20	37.2	106.9	23	77	70.3	0.33
3003	640	30	37.9	106.9	23	77	70.3	0.33
3003	640	40	37.9	106.9	23	77	70.3	0.33
4047	540	60	50	128.3	22	42	68.9	0.33

TABLE III Microhardness values of the base material and joint material for varying brazing period and joint thickness

	Average Knoop hardness numbers (HK)							
	0.00 mm joint thickness				0.254 mm (0.010 in.) joint thickness			
Brazing period	10 min	20 min	30 min	40 min	10 min	20 min	30 min	40 min
Reaction zone	78.7	71.3	46.7	49.9	66.6	60.0	62.3	60.7
Base metal	43.1	42.6	39.8	41.3	40.6	42.8	42.6	40.7

amount of aluminum-silicon eutectic matrix that forms within the reaction zone during brazing. By increasing the brazing period or decreasing the joint thickness the joint strength decreases since the amount of strong eutectic matrix formed decreases. However, this may not be solely responsible for the observed degradation of the joint strength with increasing the brazing period.

Microhardness measurements were taken to evaluate brazed region and base material strength. Tukon 200 microhardness tester with a mass of 25 grams was used to measure microhardness. Table III shows microhardness data of the base material and the brazed joints.

The microhardness of the base material was essentially constant for all joints. Therefore the strength of the base material was not affected by the brazing periods used in this study. This is in agreement with the tensile test data presented in Table II. The microhardness of the reaction zone for all joints was greater than the microhardness of the base material. Therefore, joint material is most likely stronger than the base material for all joints. This conclusion is further supported by the failure of 10 minute brazed joints. Fig. 9 shows that specimens prepared with 10 minutes brazing period failed within the base material indicating the joint was stronger than the base material. The microhardness of brazed region for joint thickness of 0.254 mm was almost constant over the range of brazing period. This could be due to presence of high Silicon content in the brazed region for these joints. However, for braze joint with 0.0 mm joint thickness, the microhardness of the joint drastically reduced for brazing period greater than 20 minutes. This could be attributed to presence of a very limited amount of eutectic microstructure in these joints and their reduction with increasing brazing period due to Silicon diffusion and base material dissolution and its entrance to the joint area. Fig. 4 indeed indicates a significant change in the microstructure of joints with 0.0 mm joint thickness and brazing period of 40 min.

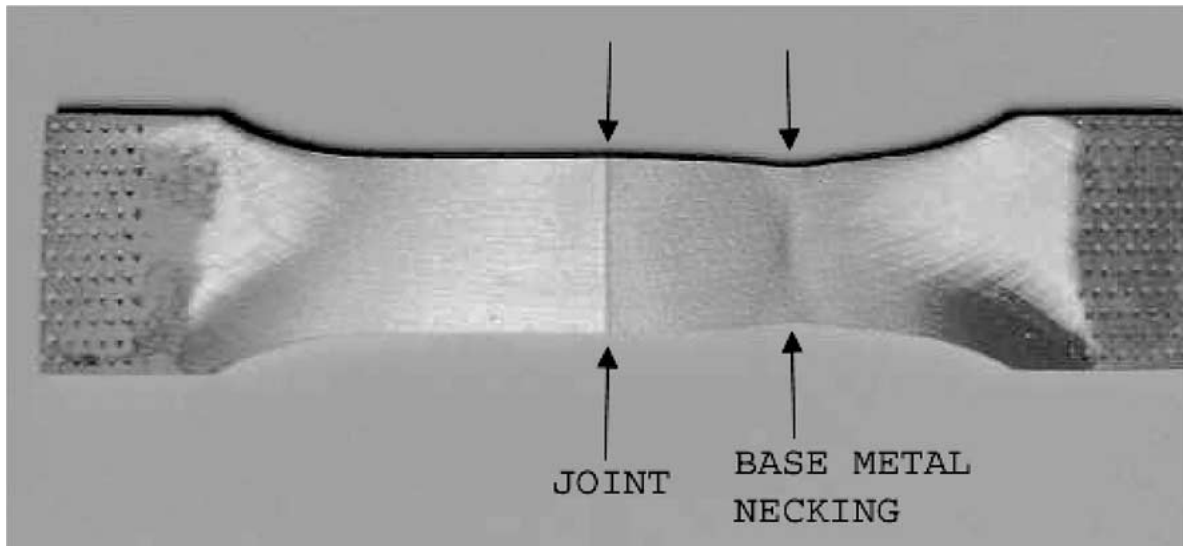

Figure 9 Typical failure mechanism of a 10 min. brazed joint with a joint thickness of 0.00 mm, showing base material yielding and necking.

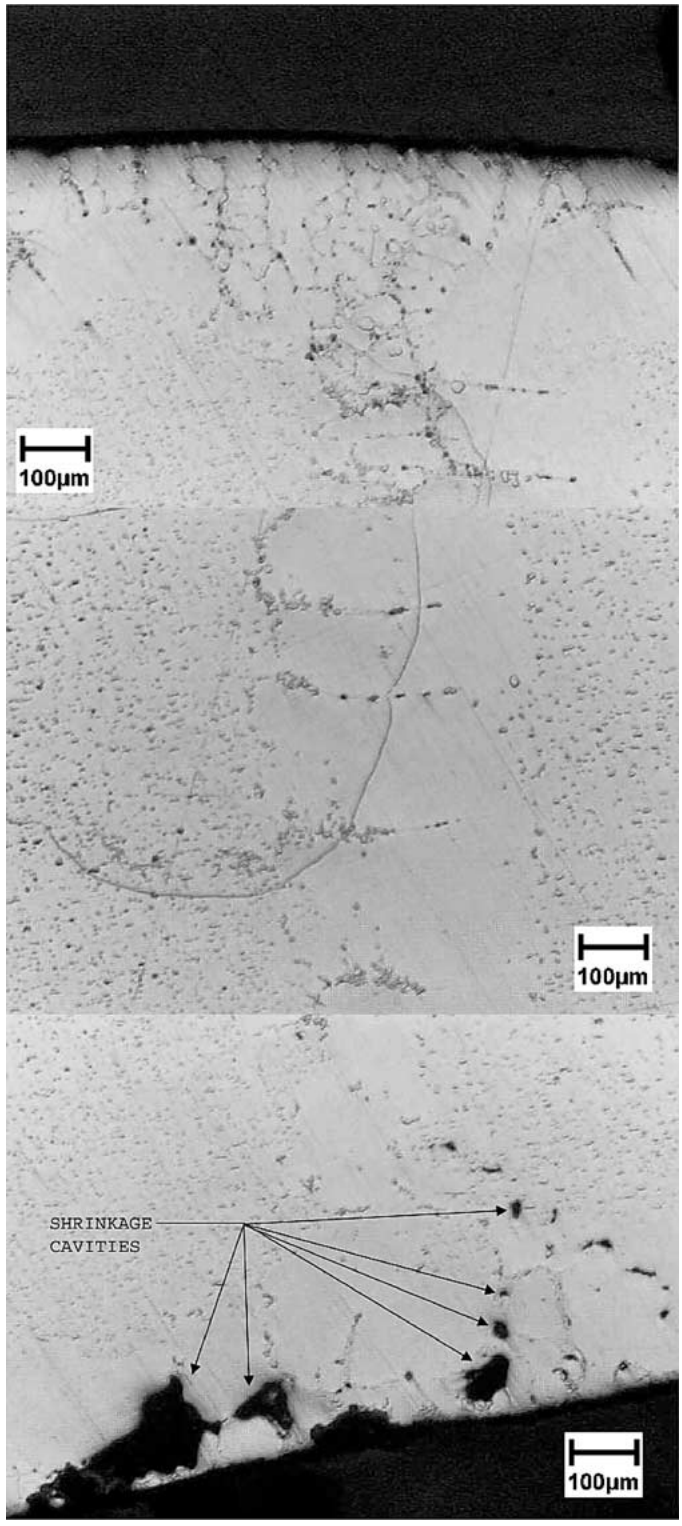

Figure 10 Photomicrograph of a brazed joint with a joint thickness of 0.00 mm and brazing period of 40 minutes, showing variation of joint microstructure through the joint and shrinkage cavities at the bottom of joint.

This could be also related to the drastic reduction in the tensile strength of these joints.

For joint with greater than 10 minutes brazing period the failure occurred within the brazing zone despite of higher microhardness value. Detailed metallographic examinations of specimens with brazing period greater than 10 minutes revealed formation of porosities in the bottom of joints, Fig. 10. Considering the phase diagram of aluminum and silicon [24], the base material could melt at operating furnace temperature of 640°C, when its silicon concentration is greater than 4%. The filler alloy initially contains approximately 12% silicon. Therefore sufficient silicon is available for base solution to occur. With an increase in silicon concentration in the bottom of the joint, the base material could melt and enter to the liquid pool of the filler material. Upon solidification of this pool, cavities can form due to its shrinkage. The combination of increasing shrinkage porosity and decreasing eutectic microstructure most likely lead to a lower failure stress of the brazed joints with brazing period greater than 10 minutes.

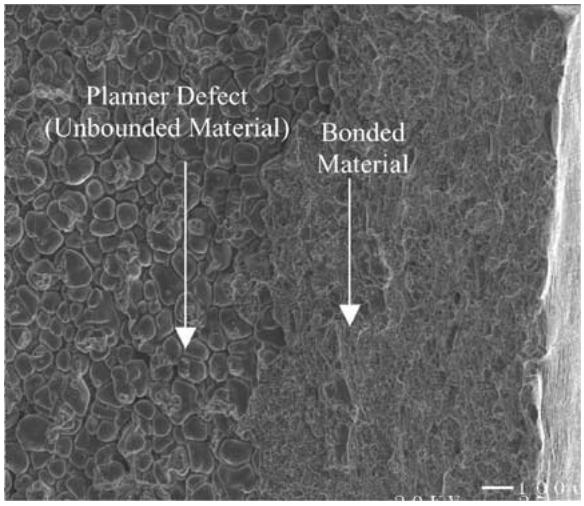

Figure 11 SEM photofractograph of the typical fracture surface of a 30 min. brazed joint with a joint thickness of 0.00 mm showing bonded and unbonded regions.

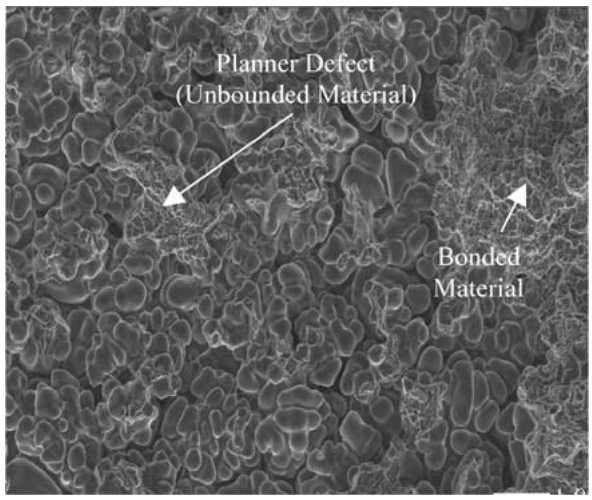

Figure 12 SEM photofractograph of the typical fracture surface of a 40 min. brazed joint with a joint thickness of 0.00 mm showing bonded and unbonded regions.

Figs 11 and 12 are SEM fractographs of typical fractured surfaces of a 30-minute and a 40 minute brazed joint with a joint thickness of 0.00 mm, respectively. The fractured joint areas show the presence of planar defects (unbonded regions) on the fracture surface. Fractography analyses revealed that as the brazing period increased the amount of planar defects also increased. The large areas of planar defects were always located on the bottom side of the joint. This could be related to an extensive dissolution of the base material in the joint region and its subsequent departure from the joint area, thus leaving voids in those regions. Furthermore, as Fig. 2 indicates, solidification initiates by formation of dendrites in the joint area. A liquid film entrapped between two dendrites could get separated from dendrites upon its solidification, leaving a planner defect in the joint area. This could be called hot tearing. Specimens with no defects also exhibited more ductile behavior than specimens with defects.

TABLE IV FEA base material and joint material mechanical properties

Material	Yield strength (MPa)	Elastic modulus (GPa)	Tangent modulus (MPa)	Poisson's ratio
Base material	37.9	70.3	1.37	0.33
Joint material 1	42.7	70.3	1.37	0.33
Joint material 2	50	70.3	1.37	0.33

3.3. Finite element analysis

Failure of a brazed joint depends on mechanical properties of the base and brazed joint as well as on the thickness of the brazed joint. For a brazed joint subjected to uniaxial loading, a complex stress field develops in the base material as well as in the brazed joint material. The failure of the joint depends on the effective stress (von Mises) stress in the base as well as brazed joint materials. In order to understand the effect of brazed joint thickness and its yield stress on the developed stress field, elastic/plastic finite element analyses were performed to obtain the stress field in brazed joints under uniaxial loading. Since brazing period, did not change the yield stress of the base material, all analyses were performed for joints with the base material yield stress of 37.9 MPa. The stress field was obtained for joints with the brazed region yield stress of 42.7 and 50 MPa and joint thickness ranging from 0.1 mm to 2.54 mm. This range covers our experimental investigation and provides further information on the effects of joint thickness on the joint strength. Both brazed region material and base material were assumed to be elastic with linear work hardening in the plastic regime. The elastic/plastic mechanical properties of the base material and joint materials which were obtained from tensile tests and used in the finite element analyses are listed in Table IV.

8-node plane stress elements were used for the finite element analyses. Fig. 13 shows a typical finite element model used for this study. Finer mesh size was used in the joint material and near the joint material/base material interface. Due to the symmetric nature of the geometry and loading, only one quarter of the structure was modeled. Each model was loaded to a uniform far field stress of 41.4 MPa.

Finite element analyses showed that a state of biaxial tension develops in the base material, and a state of biaxial tension/compression develops in the joint material. It was found that the biaxial stress field in the base material is reduced if the thickness or yield strength of the joint material is reduced. Similarly the compressive component of the biaxial stress field in the joint material is reduced if the joint thickness is increased or if the yield strength of the joint material is reduced [23]. The effects of joint thickness on the observed stress field can be justified considering the plastic deformation of the joint material. Reducing the joint thickness increases the compressive component of the biaxial stress field in the joint material, resulting in a presence of higher shear stress in the joint material. This will result in higher plastic deformation in the joint material. The increase in the plastic deformation of the joint material

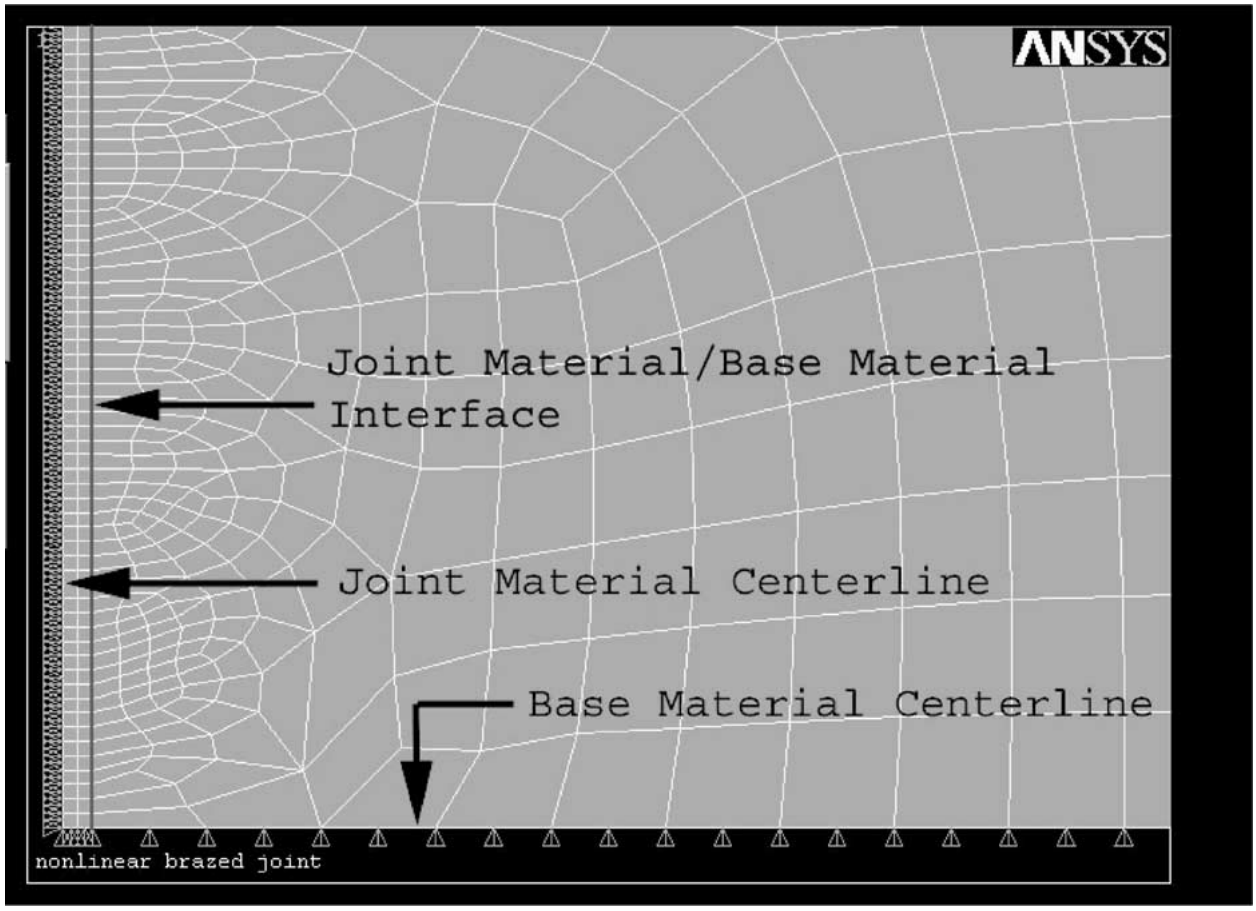

Figure 13 Finite element for a brazed joint model with 0.254 mm (0.01 in.) joint thickness with boundary conditions showing the joint material/base material interface.

reduces the constraint to the base material, thus reducing the magnitude of the biaxial component (transverse to the loading direction) of the stress field in the base material. In contrast increasing the joint thickness decreases the compressive component of the biaxial stress field in the joint material. This in return results in a reduction of the plastic deformation in the joint material. This will subsequently increase the constraint on the base material, thus increasing the biaxial component of the stress field in the base material.

A similar argument can be presented to justify the finite element analysis results on the effect of joint material yield strength on the developed transverse component of the biaxial stress field in the base material.

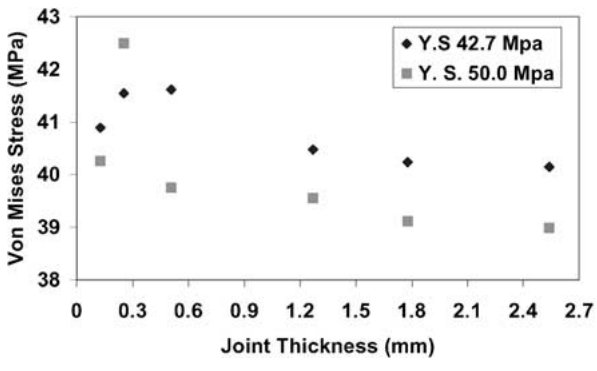

Figure 14 Variation of Von Mises stress in the base material vs. joint. thickness.

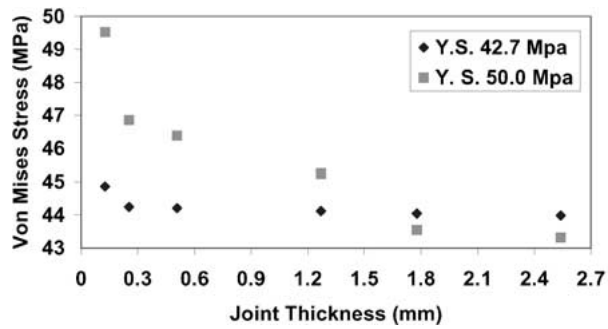

Figure 15 Variation of Von Mises stress in the joint region vs. joint thickness.

The results indicate that for joints with small joint thickness, the base material could fail prior to the joint failure. This is shown with a high Von Mises stress developed in the base material, Fig. 14. The experimental data support this conclusion, Fig. 9. Furthermore, the results indicate that joints with higher yield strength in the joint area are stronger Fig. 15. These results are also supported by experimental data where joints brazed with more filler material exhibited larger strength. The results also show for joints with yield strength of the base material lower than the brazed joint area, the joint strength in general should improve with increasing the joint thickness, provided no defects develop with further increasing the joint thickness.

4. Conclusions

Brazed butt joints consisting of two aluminum alloy 3003 plates connected by a layer of aluminum alloy 4047 filler material were manufactured. The effects of manufacturing processes such as joint thickness and brazing period on the joint microstructure, its tensile strength, micro-mechanisms of failure, and stress field in the joint when subjected to a tensile force were studied. Based on these investigations, it was found,

1. The amount of aluminum-silicon eutectic microstructure in the reaction zone decreases with increasing brazing period and decreasing joint thickness due to silicon diffusion from the joint material into the base material and dissolution of the base material.

2. The amount of shrinkage porosity in the reaction zone increases with increasing brazing period due to base material solutioning.

3. The ultimate tensile strength of a joint decreases with increasing brazing period and decreasing joint thickness because the amount of strong eutectic microstructure formed in the joint decreases and the amount of shrinkage porosity increases.

4. Shrinkage porosity is most likely the primary cause of decreased joint strength.

5. The fractured joint surfaces exhibit a more brittle type of fracture as the brazing period increases.

6. Joints with 10 minutes brazing period failed within the base material, while brazed joints with greater than 10 minutes brazing period failed within the aluminum-silicon eutectic microstructure of the reaction zone.

7. The mechanism of joint failure in the reaction zone was crack initiation at shrinkage cavity sites and crack propagation through the eutectic microstructure.

8. Finite element analysis showed that for a brazed joint with joint material yield strength greater than base material yield strength, high Von Mises stresses developed in the base material for small joint thickness, leading to the base material yielding. The Von Mises stresses decrease with increasing joint thickness. The strength of the brazed joint therefore increases with increasing joint thickness. The experimental results are in agreement with the finite element results.

References

1. The Aluminum Association Incorporated, "Aluminum Brazing Handbook," 4th edn. (1990) p. 7.
2. J. A. SCHEY, in ASM Handbook Materials Selection and Design, Vol. 20, 1997, p. 696.
3. K. SAMPATH, in ASM Handbook Materials Selection and Design, Vol. 20, 1997, p. 762.
4. N. BREDZS, *Supplement to the Welding Journal* **33** (1954) 545.
5. W. G. MOFFATT and J. WULFF, *ibid.* **42** (1963) 115.
6. H. J. SAXTON, A. J. WEST and C. R. BARRETT, *Metallurgical Transactions* **2**(4) (1971) 999.
7. A. J. WEST, H. J. SAXTON, A. S. TETELMAN and C. R. BARRETT, *ibid.* **2**(4) (1971) 1009.
8. H. J. SAXTON, A. J. WEST and C. R. BARRETT, *ibid.* **2**(4) (1971) 1019.
9. K. SASABE, *Quarterly Journal of the Japan Welding Society* **7**(2) (1989) 98.
10. F. P. L. KAVISHE and T. J. BAKER, *Material Science and Technology* **6** (1990) 176.
11. S. SATO, M. SUKIMOTO, S. ITONAGA and T. HONDA, *Journal of Japan Institute of Light Metals* **43**(9) (1993) 478.
12. M. A. MILLER, *Supplement to the Welding Journal* **20** (1941) 472.
13. *Idem.*, *ibid.* **22** (1943) 596.
14. *Idem.*, *ibid.* **25** (1946) 102.
15. J. R. TERRILL, *ibid.* **45** (1966) 202.
16. R. A. WOODS and I. B. ROBINSON, *ibid.* **53**(10) (1974) 440.
17. P. SHARPLES, *Welding Journal* **54**(3) (1975) 164.
18. E. B. GEMPLER, *Supplement to the Welding Journal* **55**(10) (1976) 293.
19. A. M. NIKITINSKII *et al*., *Welding Production* **26**(6) (1979) 38.
20. D. J. SCHMATZ, *Supplement to the Welding Journal* **62**(10) (1983) 267.
21. D. R. MILNER, *British Welding Journal* **15** (1958) 90.
22. ASTM Designation E 8-99, 1999 Annual Book of ASTM Standards, Section 3, Vol. 03.01 (ASTM, 1999) p. 57.
23. M. LOCKWOOD, M.S. thesis, Department of Mechanical, Industrial and Manufacturing Eng., Northeastern University, Boston, MA 02115, June 2001.
24. ASM Handbook,"Binary Alloy Phase Diagrams," Vol. 3, 1992, p. 2.44.

Received 25 June 2001
and accepted 17 April 2002